



Calcein and calcein–Ag films under vapor exposure: Sensing properties and reversible film restructuring

I. Kruglenko^{a,*}, J. Burlachenko^a, S. Kravchenko^a, P. Lytvyn^a, E. Manoilov^a, M. Slabkovska^b

^a V. Lashkaryov Institute of Semiconductor Physics, NAS of Ukraine, Ukraine

^b V.M.Glushkov Institute of Cybernetics, NAS of Ukraine, Ukraine

ARTICLE INFO

Available online 24 September 2012

Keywords:

Calcein
Restructuring
Swelling
Reverse swelling
Nanoactuators
Silver nanoparticles

ABSTRACT

We studied the adsorption properties of organic and organic-inorganic films based on the dye calcein. Embedding of silver nanoparticles increases film sensitivity to some analytes (in particular, sensitivity to ethanol increases by about 30%). Both films demonstrate high sensitivity to water vapor, response of about 7000 Hz for a quartz crystal microbalance sensor. Our investigations showed that essential restructuring of films and increase in their thickness occurs in the course of adsorption of water molecules. These changes are reversible: after drying, the sensor response reverts to zero and the film structure is fully restored. The value and reversibility of changes occurring because of adsorption processes at the surfaces of calcein and calcein–Ag films make these materials very promising for application not only in sensorics but also when developing nanoactuators as well.

© 2012 Elsevier B.V. All rights reserved.

1. Introduction

The processes occurring at adsorption of vapors of various analytes onto the surfaces of thin films attract attention of researchers dealing with analytical chemistry, solid state physics and catalysis. The origins of such processes are interactions between a gas component and the reactive groups at the film surface. Understanding the mechanisms of adsorption and its effect on the material properties is of importance for development of novel technologies in such areas as micro- and nanoelectronics, medicine and sensorics. Of particular interest are the reversible processes related to physical adsorption since they may serve as basis for operation of sensors and actuators with long service life. From this viewpoint the organic materials (in particular, dyes) are preferred.

The organic dyes are rather widely used in sensorics as sensitive coatings, first of all, in optical sensors. In addition to their optical properties (intense adsorption and fluorescence bands) these materials demonstrate wide adsorption properties. Indeed, the molecular structure of dyes involves functional groups able to make bonds of different nature (hydrogen, van der Waals, π -stacking etc.) with various gas molecules. Additional adsorption centers appear at organization of molecules into a film. Depending

on the type of the film (crystalline, amorphous, polymer), the centers formed at the surface are related to interaction of neighboring molecules and their clusters as well as to defects of different nature [1]. A diversity of adsorption centers as well as extreme flexibility of such materials related to a possibility of varying their properties over wide limits by replacement of their functional groups and formation of hybrid materials on their basis makes dyes very promising materials.

Calcein is an organic dye that is widely used in different areas, in particular, biology and medicine. It serves as fluorescent marker [2–6], in ophthalmology (for fundus angiography, macular surgery etc.) [7–9], in biology (as cell viability marker, in fluorescence microscopy etc.) [10–12], as well as investigation of features of bone tissue [13,14]. Calcein-based nanosensors are used to detect metal ions, for example, in blood serum [2,5,15–17]. However, there is not enough information in literature on the application of calcein films. As a rule, calcein and its derivatives are used as a part of composite films based on inorganic and organic (in particular, polymer) materials [17,18].

In our previous work [19] we studied the adsorption properties of a thermally deposited calcein film (TDCF). The film proved to be an interesting and promising material for chemical sensors, in particular, humidity sensors. The process of thermal deposition of calcein presents some technical complexities and it is difficult to achieve the suitable rate of film properties repeatability. Taking into account the potential interest of practical application of calcein-based devices, in the present work we investigate the properties of calcein films obtained from a solution.

* Correspondence to: ISP, NAS of Ukraine, Nauki av. 41, 03028 Kiev, Ukraine. Tel.: +380 44 5255626.

E-mail addresses: kruglenko@yahoo.com, kruglen@isp.kiev.ua (I. Kruglenko).

Embedding nanoparticles in organic dyes can result in hybrid materials with improved (and new) properties [20–22]. Use of mixed layers based on organic dyes with noble metal nanoparticles is rather often mentioned in the literature on sensorics [23]. In such cases, the nanoparticles serve to enhance fluorescence – the so-called metal-enhanced fluorescence effect [24–26]. Interaction between the molecular excitons in dyes and plasmons in nanoparticles leads to appearance of new electron states at the material surface. This may essentially enrich the adsorption properties of the material. We have made a hybrid material based on calcein and silver nanoparticles.

The preliminary data obtained for TDCF indicate possible changes of the film's physical characteristics (in particular, its morphology and thickness) owing to adsorption. The sensor responses, being reversible and reproducible, were considerably high. So understanding the mechanisms of the above changes seems to be of great practical importance. That is why we gave much attention in this work to study of reversible change of film structure under exposure to water vapor.

2. Materials and methods

2.1. Materials

Calcein (Sigma), sodium hydroxide (Macrochim) and silver nitrate (Macrochim) were used as received. The nylon bottle-top filter system with the pore size of 0.2 μm (Corning) was obtained from Fisher. Ultra pure water with resistivity over 18.3 $\Omega\text{ cm}$ was obtained from a Millipore Milli-QTM columns system provided with a Millipak filter of 0.22 μm pore size at the outlet.

2.2. Preparations of silver nanoparticles and calcein–Ag

Silver nanoparticles capped with calcein were prepared by reduction of AgNO_3 . Briefly, 10 ml of 2.5 mM of calcein and 1.3 ml of 0.1 M NaOH were added to 40 ml of boiling water, and then 0.31 μl of 0.1 M AgNO_3 was added under vigorous stirring. A dark green color appeared and intensified after a couple of minutes. The mixture was then kept at boiling for 2–3 min, cooled and filtered through 0.2 μm nylon bottle-top filter system to yield 32 ± 9 nm silver nanoparticles ($v_{\text{max}}=404$ nm). The solution was ready for use immediately after preparation and remained stable for months.

The sensitive layers were deposited onto the surfaces (quartz resonators as elements of mass sensitive sensors, silicon plates for optical microscopy and AFM characterization, TEM sample support meshes) using the droplet technique. A calcein solution as well as that of nanoparticles in calcein (14 μl droplet of solution) was deposited with a dispenser onto the horizontal surface of the substrates under investigation that were cleansed of contaminants. The film obtained was dried in a clean box at room temperature for 5 h.

2.3. Quartz crystal microbalance (QCM)

In our investigations we used sensors based on quartz piezoelectric resonators (AT-cut quartz plate with silver electrodes deposited on the opposite sides of the plate) with resonance frequency of 10 MHz. To excite resonator vibration as well as measure and register change of vibration frequency, we used oscillators, a frequency meter and software developed at the V. Lashkaryov Institute of Semiconductor Physics of the National Academy of Sciences of Ukraine [27]. The sensors were placed in a flow-through measuring cell. A liquid analyte was in a flask. A molecular flow from the surface of materials under investigation

was entrained by a gas-carrier (argon) with a constant speed (60 ml/min) at constant room temperature (25 $^{\circ}\text{C}$), thus forming gas sample. The concentrations of analytes were close to saturation level. The responses of a quartz resonator without sensitive coating to all analytes under investigation did not exceed 10 Hz.

2.4. Optical microscopy, TEM, AFM, fluorescence

The surface topology was studied using an optical microscope Nu-2E (Carl Zeiss) equipped with a 8 megapixel camera Canon EOS 350D. TEM investigations were performed using a transmission electron microscope JEOL JEM 1011, at an accelerating voltage of 100 kV.

AFM measurements were performed with NanoScope IIIa Dimension instrument (Digital Instruments/Bruker, USA). To measure the influence of water vapor on the film thickness and surface topology, the samples (calcein and Ag-calcein films on the silicon plates) were maintained in saturated water vapor for 10 min. Then the samples were placed in the measurement chamber.

The absorption spectra were taken with a spectrophotometer Specord M40 in 300–900 nm wavelength range.

Investigation of the fluorescence spectra was performed using a setup for registration of faint light, with time division in the photon-counting mode. Fluorescence was excited by radiation from an N_2 laser ($\lambda=337$ nm, pulse duration $\tau_p=8$ ns). The minimal strobe pulse interval τ during which photon accumulation took place was 250 ns. The sequential fluorescence spectra were registered with a measuring strobe pulse to laser pulse delay. The spectra of rapid ($\tau < 250$ ns) fluorescence component were measured by making the leading edge of the measuring strobe pulse of minimal duration coincident with that of the pulse from the N_2 laser. The fluorescence relaxation times below 50 ns were estimated using an oscilloscope [28].

3. Results and discussion

We showed previously that TDCF demonstrates extremely high sensitivity to water vapor and much lower sensitivity to other analytes [19]. Similar properties were demonstrated by a calcein film obtained from a solution. This result is important from the viewpoint of practical applications because the procedure of thermal deposition of calcein involves considerable technological difficulties, while obtaining calcein films from a solution is simple and does not require additional equipment. Our further investigations were made using films from a solution.

Fig. 1a presents a TEM photograph of silver nanoparticles synthesized in a calcein solution. The average size of spherical particles was 25 ± 5 nm. The nanoparticle size histogram (Fig. 1b) was built from several TEM photographs.

Shown in Fig. 2 are the absorption spectra of calcein solution and colloidal solution of silver nanoparticles in calcein. The spectrum of calcein solution peaks at 490 nm which is characteristic of this material. Another spectrum has a new peak at 410 nm that corresponds to absorption by silver nanoparticles [29].

The fluorescence spectra of the calcein and calcein–Ag films taken in air and in water vapor are shown in Fig. 3. Without water vapor, the fluorescence spectra overlap a wide range of wavelengths, from 400 to 900 nm, with a broad maximum at about 500 nm. The maximal fluorescence was observed at $\lambda=509$ nm with intensity of 4 arb. u. for calcein and 6 arb. u. at $\lambda=520$ nm for the calcein–Ag film. The values of fluorescence relaxation time were rather close for all the samples under investigation and equaled about 150–200 ns.

In the water vapor, fluorescence increased by about five times, the spectral peak becomes pronounced more clearly, and a

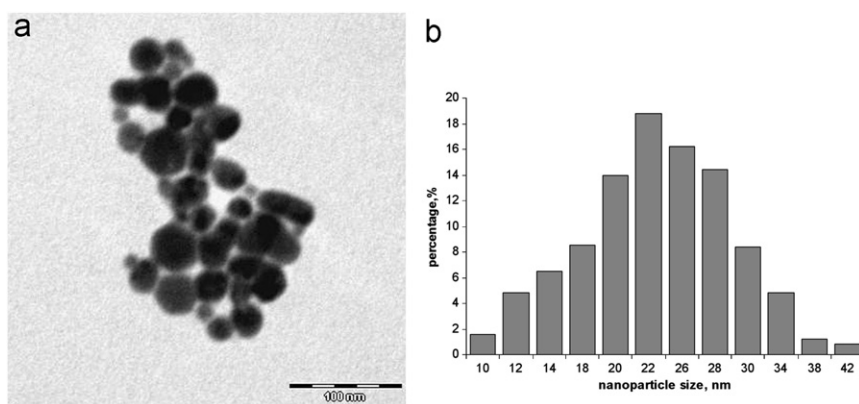


Fig. 1. TEM photograph of silver nanoparticles (a) and their size distribution (b).

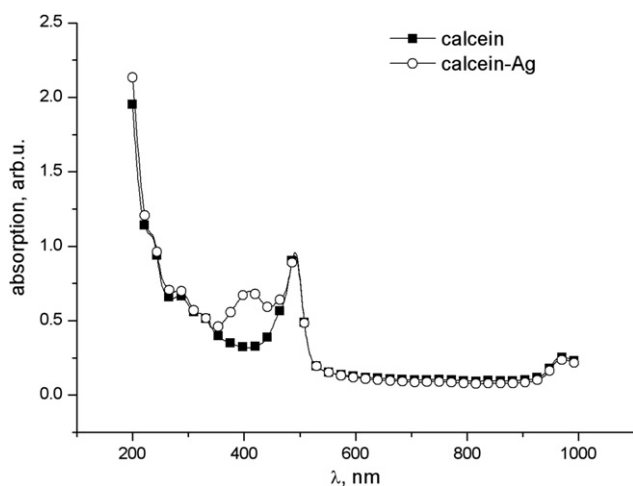


Fig. 2. The absorption spectra of water solutions of calcein and silver nanoparticles synthesized in calcein solution.

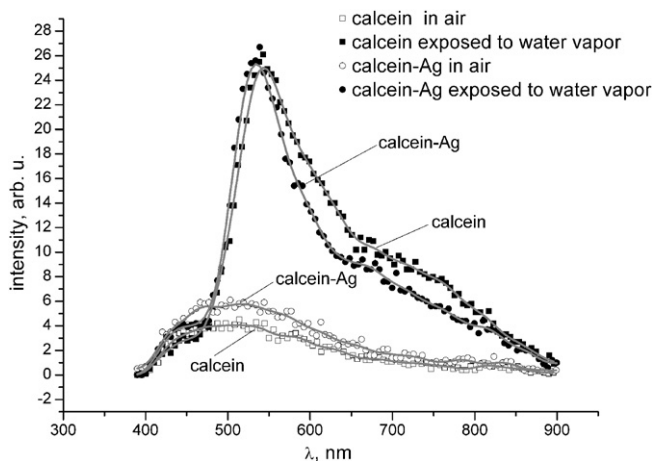


Fig. 3. The fluorescence spectra of calcein and calcein-Ag films in air and water vapor.

shoulder appears in the wavelength range of 650–800 nm. In that case, the maximal fluorescence of calcein is observed at $\lambda=547$ nm with intensity of 25.0 arb. u., while for a calcein-Ag film it is observed at $\lambda=532$ nm with intensity of 25.3 arb. u.

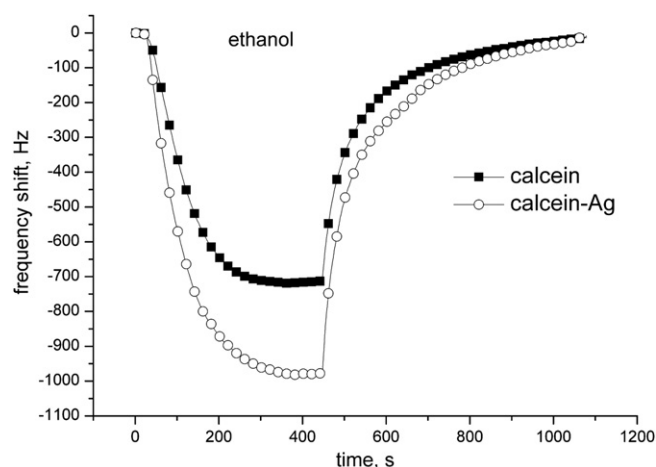


Fig. 4. The responses of QCM sensors coated with calcein and calcein-Ag films to ethanol vapor.

Thus, under action of water vapor, one may observe not only essential intensification of fluorescence but also shift of spectral peaks as well. This shift (towards longer wavelengths) is 40 nm for calcein and 12 nm for calcein-Ag. Therefore, the calcein films can serve as basis for fabrication of fluorescent sensors. Intensification of fluorescence indicates formation of hydrogen bonds between the carboxyl groups and water molecules.

Fig. 4 shows how the QCM sensors whose coatings are films obtained from solution of calcein and colloidal solution of silver nanoparticles synthesized in calcein respond to the ethanol vapor. One can see that embedding of silver nanoparticles increases sensitivity of ethanol by 30%. The sensor responses are reversible and reproducible. There were performed about 100 measurements with the same calcein and calcein-Ag films during 1 year and 2 months. The response amplitude varied to $\pm 3.5\%$ for ethanol and $\pm 4\%$ for water vapors. In the course of cleaning the response curve returned to zero with accuracy ± 10 –20 Hz. Taking into account high concentrations of analytes, calcein and calcein-Ag films can be considered as stable and long-life organic coatings.

The responses of the same sensors to water vapor are presented in Fig. 5. In this case, embedding of silver nanoparticles did not lead to considerable effect. It was noted above that the amplitude of sensor responses to water is extremely high. Besides, the character of adsorption curves is essentially different than in the case of ethanol adsorption. For both films (calcein and calcein-Ag), after a certain maximum response is reached

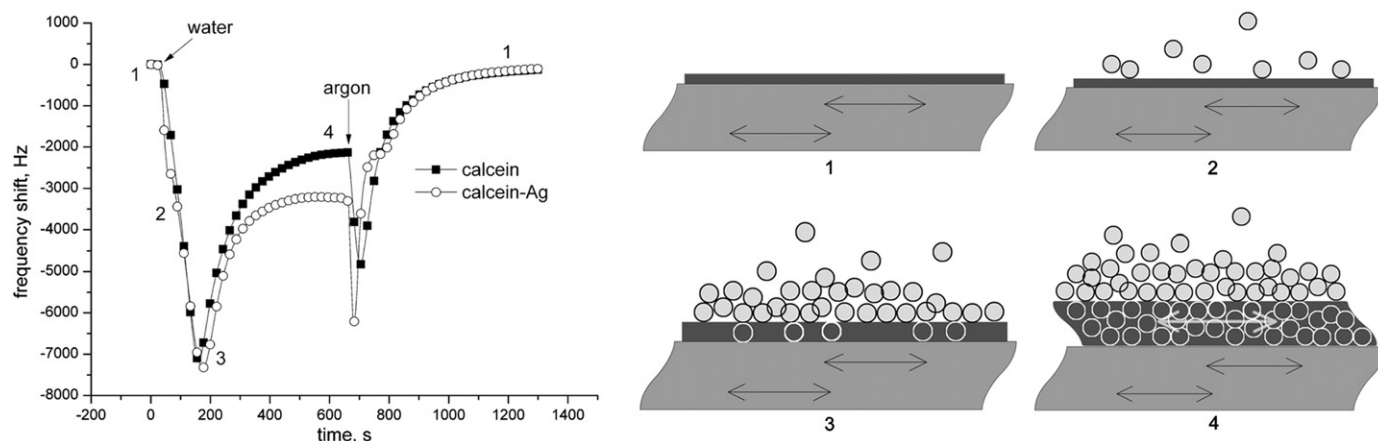


Fig. 5. (At the left) – The responses of QCM sensors coated with calcein and calcein–Ag films to water vapor. (At the right) – The schematic of film swelling process at different stages of water molecules adsorption.

(7150 Hz for the first film and 7340 Hz for the second film), the adsorption curve begins to rise and then flattens out (2200 Hz for the first film and 3200 Hz for the second film). In the course of cell cleaning (blowing-through with pure argon), the response practically returns to its maximal value, and then goes to zero.

Such sensor behavior may be explained in the following way. An AT-cut quartz plate (that serves as transducer) makes shear vibrations. This situation is denoted in Fig. 5 by 1. As the plate mass increases due to adsorption of analyte molecules onto the sensitive layer deposited on one of the electrodes, the resonance frequency of system vibrations goes down, and this is a measured sensor response (portions 1–2–3 of the curve, schematic 2). As the maximum is reached, the processes of diffusion into the film begin to play an essential role (schematic 3). Starting from this moment, considerable film thickness and/or essential difference between the viscous-elastic properties of the film and electrode become the dominant factors affecting the frequency of vibrations. As the sensitive layer thickness increases because of water molecules diffusion in the film, the sensor begins to vibrate as a complex vibrating system (portion 3–4 of the curve, schematic 4) rather than a whole. If the saturated water vapor is replaced with pure argon, then rapid desorption of water molecules from the surface occurs, reverse swelling begins and the frequency shift reverts to its previous value of 6000 Hz. The film thickness decreases, thus leading to restoration of the dominant effect of adsorbate mass on the vibration frequency (schematic 3). After this, the frequency shift gradually returns to zero in the course of continuing desorption.

Similar behavior of the QCM sensor response curve was reported for example in [30]. Authors studied the adsorption of cells on a solid surface of QCM electrode. In the course of adsorption, first, the frequency decreased, then it started to increase continuously and after some time exceeded the initial sensor frequency. It was shown by the results of measuring of the maximal oscillation amplitude and the transient decay time constant that positive frequency shift is concerned with the changes of viscoelastic properties of the adsorbate on the electrode's surface.

Restructuring the sensitive layer surface in the course of adsorption–desorption is quite possible for molecular crystals where intermolecular bonding is relatively weak, and interaction with adsorbate may be of the same order as in between the molecules of material [1]. We believe, however, that such essential changes (with further material returning to its original state) are a unique phenomenon.

The restructuring process for a calcein–Ag film is shown in Fig. 6. A set of experiments were made on a silicon sample with a

calcein–Ag film in water vapor using a microscope. The photograph 6.1 shows the initial (before exposure to water vapor) sample surface; and the photograph 6.5 shows the sample surface after drying. The times of sample exposure to water vapor are given under the photographs 6.2–6.4.

The graph in Fig. 6 shows the evolution of surface fractal dimension on each stage of experiment (the numbers on the graph correspond to the numbers of photographs). The fractal dimension D was calculated for each photograph (6.1–6.5) using the triangulation method [31]. It should be noted that calcein–Ag film has fractal structure of the surface on each stage of experiment.

In the course of water molecules adsorption, nonuniform surface with a developed relief gradually transforms into smooth uniform one. The variations of the surface begin at the film periphery and progressively spread towards the center. The most interesting fact is that, even after cardinal changes, the surface returns to its initial state after drying. The surface fractal dimension evolution shown in Fig. 6 proves the film behavior, the fractal dimension decreases in the course of water adsorption and returns to the initial value after cleaning the surface.

The calcein film (without silver nanoparticles) subjected to water vapor demonstrates similar behavior, with returning to the initial state after drying.

AFM data demonstrating the surface changes caused by water adsorption are presented in Fig. 7 (a – calcein film, initial state; b – calcein–Ag film, initial state; c – calcein film after 10 min of water vapor exposure; d – calcein–Ag film after 10 min of water vapor exposure) On the right side of each picture there is a scratch made for thickness measurements. Calcein–Ag film has more developed surface with complicated relief while calcein film is more smooth (see Fig. 7a and b). The difference in surface area may be one of the reasons why calcein–Ag film demonstrates bigger responses to ethanol and water (see Figs. 4 and 5).

After 10 min of water exposure increase in films thickness and smoothing of their surfaces are observed (see Fig. 7c and d). The effect of film surface smoothing is much stronger for calcein–Ag film (compare Fig. 7c and d). The change in average film thickness caused by water exposure is 47% for calcein film and 33% for calcein–Ag. It should be noted that AFM measurements were performed not *in situ* as it was in the case of QCM measurements. This means that the concentration of adsorbed water molecules in this case is less than that for the QCM measurements. So, the real effect of calcein and calcein–Ag films exposure in water vapor of high concentration is even stronger than shown in Fig. 7.

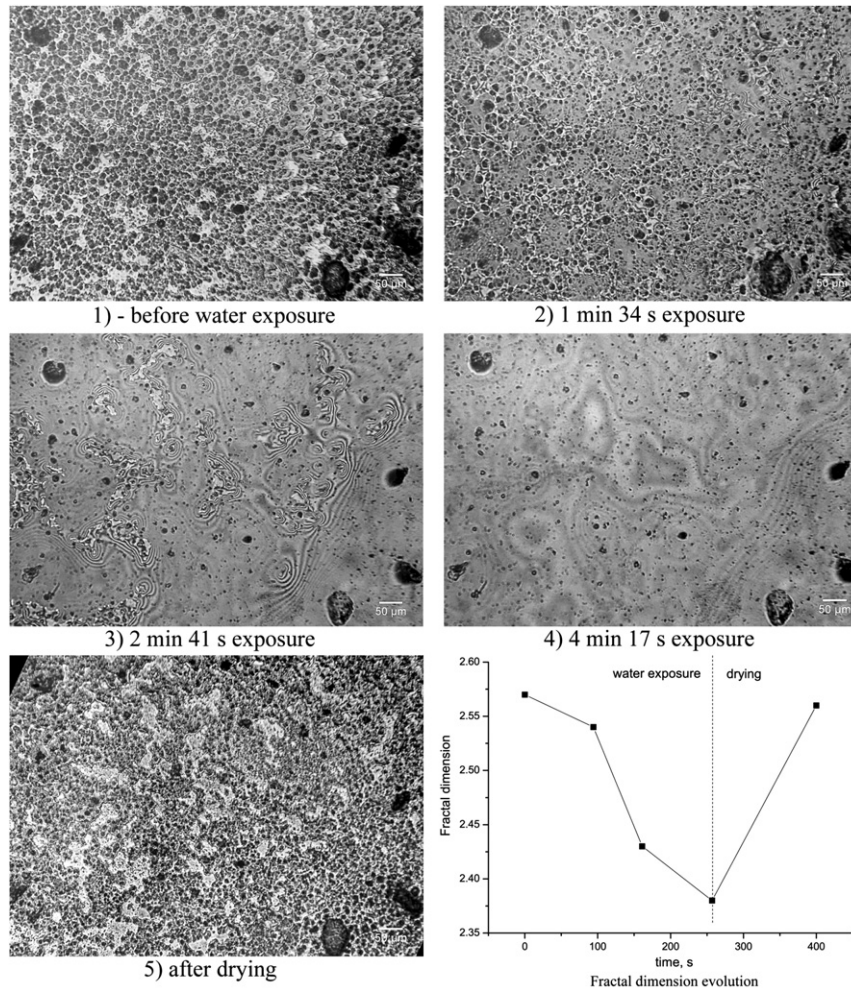


Fig. 6. The photographs of calcein–Ag film surface taken at different stages of exposure to water vapor and after drying. The graph shows the fractal dimension evolution of the same surface during its exposure to water vapor. The numbers on the graph correspond to the numbers of photographs.

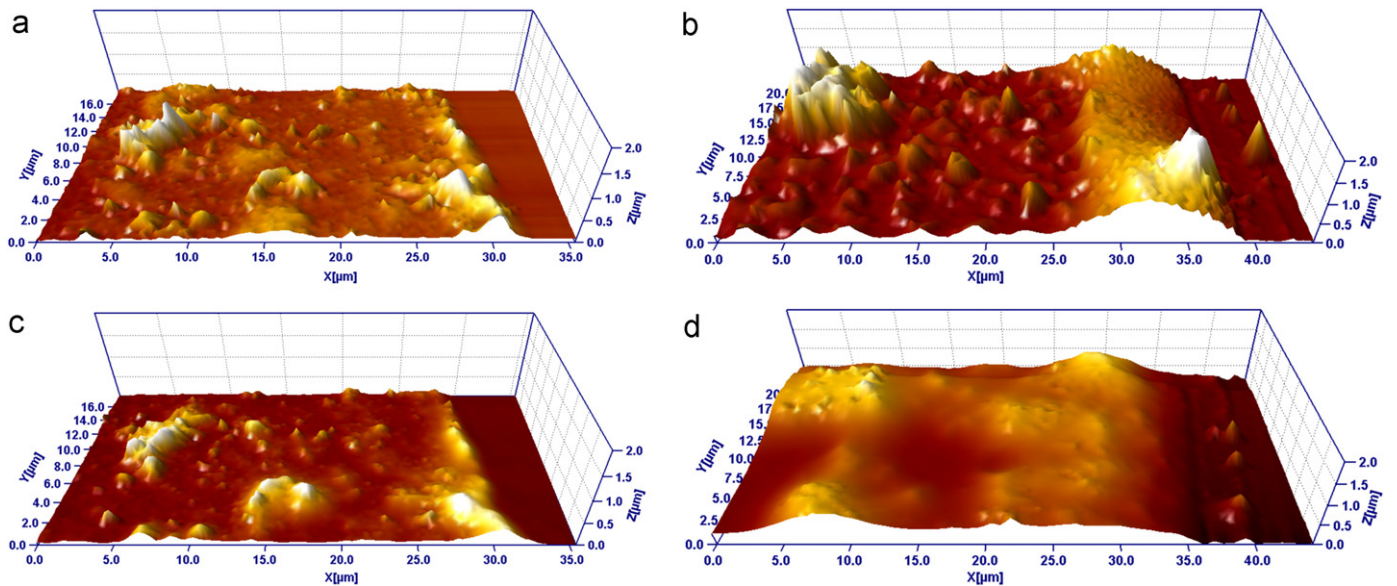


Fig. 7. AFM images of calcein and calcein–Ag films. a – calcein film, initial state; b – calcein–Ag film, initial state; c – calcein film after 10 min of water vapor exposure; d – calcein–Ag film after 10 min of water vapor exposure.

4. Conclusions

The calcein films obtained from solution demonstrated even more interesting properties than TDCFs. Their response to water is of the same order as that of TDCFs, while the response to ethanol is even bigger. Exposure of the films to water vapor leads to considerable changes in the fluorescence spectra, their intensity increases by five times. The water adsorption curves obtained using a mass-sensitive QCM sensor are of uncommon form; we believe that this is related to changes in film thickness and viscous-elastic properties. The optical microscope measurements and AFM data showed that essential film restructuring occurs under action of water vapor. The unique feature is that after drying the films return to their initial state. The results obtained may be of interest not only when using calcein films in chemical sensors but also for development of nanoactuators as well.

Acknowledgments

The authors are grateful to B. Snopok for his interest in this work and P. Boltovets for her help in measuring the absorption spectra of the materials under investigation. Authors would like to thank prof. Yu. M. Shirshov for his help and advices.

References

- [1] M. Pope, C.E. Swenberg, *Electronic Processes in Organic Crystals and Polymers*, Oxford University Press, 1999.
- [2] Y. Wang, J.M. Baten, S.P. McMaughan, D.R. Bobbitt, *Microchem. J.* 50 (1994) 385–396.
- [3] K.E.S. Dean, G. Klein, O. Renaudet, J.-L. Reymond, *Bioorg. Med. Chem. Lett.* 13 (2003) 1653–1656.
- [4] M.H. Noire, B. Dureault, *Sens. Actuators B* 29 (1995) 386–391.
- [5] X. Hun, Z. Zhang, *Microchim. Acta* 159 (2007) 255–261.
- [6] S. Sofou, J.L. Thomas, *Biosens. Bioelectron.* 18 (2003) 445–455.
- [7] M. Oncel, B. Khoobehi, G.A. Peyman, *Int. Ophthalmol.* 14 (1990) 245–250.
- [8] T.L. Jackson, L. Griffin, B. Vote, J. Hillenkamp, J. Marshall, *Exp. Eye Res.* 81 (2005) 446–454.
- [9] M.R. Golshani, B. Khoobehi, G.A. Peyman, *Int. Ophthalmol.* 17 (1993) 349–353.
- [10] J. Uggeri, R. Gatti, S. Belletti, R. Scandroglio, R. Corradini, B.M. Rotoli, G. Orlandini, *Histochem. Cell Biol.* 122 (2004) 499–505.
- [11] P. Grieshaber, W.A. Lagrèze, Ch. Noack, D. Boehringer, J. Biermann, *J. Neurosci. Methods* 192 (2010) 233–239.
- [12] M. Wartenberg, H. Acker, *Micron* 25 (1995) 395–404.
- [13] S.J. Du, V. Frenkel, G. Kindschi, Y. Zohar, *Dev. Biol.* 238 (2001) 239–246.
- [14] M. Hori, H. Takahashi, T. Konno, J. Inoue, T. Haba, *Bone* 6 (1985) 147–154.
- [15] L.C. Taylor, M.B. Tabacco, J.B. Gillespie, *Anal. Chim. Acta* 435 (2001) 239–246.
- [16] J. Kim, X. Wu, M.R. Herman, J.S. Dordick, *Anal. Chim. Acta* 370 (1998) 251–258.
- [17] Y. Sadaoka, Y. Sakai, Y. Murata, *Sens. Actuators B* 13–14 (1993) 420–423.
- [18] D. Chen, M.D. Luque de Castro, M. Valcárcel, *Anal. Chim. Acta* 234 (1990) 345–352.
- [19] I. Kruglenko, Yu. Shirshov, J. Burlachenko, A. Savchenko, S. Kravchenko, M.G. Manera, R. Rella, *Talanta* 82 (2010) 1392–1396.
- [20] C. Hanisch, N. Ni, A. Kulkarni, V. Zaporozhchenko, T. Strunskus, F. Faupel, *J. Mater. Sci.* 46 (2011) 438–445.
- [21] N. Terasaki, N. Yamamoto, T. Hiraga, I. Sato, Y. Inoue, S. Yamada, *Thin Solid Films* 499 (2006) 153–156.
- [22] M. Ihara, M. Kanno, S. Inoue, *Physica E* 42 (2010) 2867–2871.
- [23] Sh.-Zh. Tan, Y.-J. Hu, F.-Ch. Gong, Zh. Cao, J.-Y. Xia, L. Zhang, *Anal. Chim. Acta* 636 (2009) 205–209.
- [24] A.I. Dragan, K. Golberg, A. Elbaz, R. Marks, Y. Zhang, Ch.D. Geddes, *J. Immunol. Methods* 366 (2011) 1–7.
- [25] A.I. Dragan, E.S. Bishop, J.R. Casas-Finet, R.J. Strouse, M.A. Schenerman, C.D. Geddes, *Anal. Biochem.* 396 (2010) 8–12.
- [26] J. Geng, J. Liang, Y. Wang, G.G. Gurzadyan, B. Liu, *J. Phys. Chem. B* 115 (2011) 3281–3288.
- [27] B. Snopok, I. Kruglenko, *Sens. Actuators B* 106 (2005) 101–113.
- [28] E.B. Kaganovich, E.G. Manoilov, I.R. Basylyuk, S.V. Svechnikov, *Semiconductors* 37 (2003) 336–339.
- [29] T. Dadosh, *Mater. Lett.* 63 (2009) 2236–2238.
- [30] C.G. Marxer, M.C. Coen, T. Greber, U.F. Greber, L. Schlapbach, *Anal. Bioanal. Chem.* 377 (2003) 578–586.
- [31] C. Douketis, Zh. Wang, T.L. Haslett, M. Moskovits, *Phys. Rev. B* 51 (1995) 22–31.